Dalton Transactions

ROYAL SOCIETY OF CHEMISTRY

PAPER

View Article Online
View Journal | View Issue

Cite this: *Dalton Trans.*, 2026, **55**, 4525

Efficient synthesis of cyclic carbonates and oxazolidinones by simple zinc guanidinato complexes

Carlos Ginés, [a] Blanca Parra-Cadenas, [a] David Elorriaga, [b] Daniel García-Vivó, [c] Rafael Fernández-Galán,[a] Alberto Ramos [a] and Fernando Carrillo-Hermosilla *[a]

Received 19th January 2026,
Accepted 19th February 2026

DOI: 10.1039/d6dt00139d

rsc.li/dalton

Guanidinato-stabilized zinc complexes, featuring or lacking additional functionalities, were synthesized through the reaction between guanidine derivatives, specifically $(iPrHN)_2CNR$ (R = Ph, 2-FC_6H_4, 2-$Ph_2PC_6H_4$, 2-$PhSC_6H_4$), and $ZnMe_2$. The simple complex [ZnMe{(iPrN)(iPrNH)CNPh}] has been demonstrated to be a highly efficient catalyst for the synthesis of cyclic carbonates *via* the coupling of epoxides and CO_2 at atmospheric pressure in neat conditions, as well as the production of oxazolidinones through the coupling of epoxides and isocyanates, in 2-MeTHF as a sustainable solvent.

Introduction

The evolution of the global consumer market for raw materials and its impact on the environment is steering us towards a circular economy. This economy focuses on the efficient utilization of waste coming from the production of consumer goods or the goods themselves after use. Specifically, the development of new synthesis processes, starting from renewable raw materials, with sustainable reaction conditions and specific selectivities, is a significant challenge for chemical research.

One of the main wastes that is seriously affecting the environment is CO_2, which comes from the growing consumption of fossil fuels for energy over more than a century. At this point, although the capture and utilization of CO_2 will not significantly mitigate the emissions of this greenhouse gas, we should not overlook the possibilities it offers as an abundant and non-toxic raw material for the production of widely used chemicals. Thus, beyond its traditional transformation into commodities such as fertilizers, or its use in the food industry, there has been a recent shift towards its use as a raw material for fine chemicals and solvents.[1]

However, due to the thermodynamic stability and kinetic inertness of CO_2, its efficient utilization is challenging. The process of catalytically integrating CO_2 into another molecule appears to be a practical solution. Among the processes that do not involve CO_2 reduction, one of the most prominent fixation methods is the creation of cyclic organic carbonates through cycloaddition to epoxides. This reaction presents an alternative route to carbonates, with higher atomic efficiency compared to the traditional process that requires the formation and use of phosgene. Cyclic carbonates are stable compounds that serve multiple purposes, including acting as potential green solvents or as chemical intermediates to be transformed into more sophisticated scaffolds, making them an excellent solution for the much-desired valorization of waste CO_2. At this point, numerous efficient catalysts have been formulated for the cycloaddition of CO_2 and epoxides, including organometallics and organocatalysts.[2]

On the other hand, oxazolidinones, nitrogen-containing analogues of cyclic carbonates, are also important heterocyclic motifs found in commercial pharmaceuticals as antimicrobials active against multiple-resistant Gram-positive pathogens, including methicillin-resistant *Staphylococcus aureus*, penicillin-resistant streptococci, and vancomycin-resistant enterococci, of which Linezolid is the most recognized commercial brand.[3] These compounds also have a range of other applications such as chiral auxiliaries or ligand precursors.[4]

These substances are obtained through multi-step processes, which involve a non-catalytic coupling between a carbamate and chloropropanediol or an epoxide, in the presence of stoichiometric amounts of bases, as the central step to form the oxazolidinone core.[3c] Therefore, the development of new

[a]*Departamento de Química Inorgánica, Orgánica y Bioquímica-Centro de Innovación en Química Avanzada (ORFEO-CINQA), Facultad de Ciencias y Tecnologías Químicas, Universidad de Castilla-La Mancha, 13071 Ciudad Real, Spain. E-mail: Fernando.Carrillo@uclm.es*
[b]*Departamento de Química Inorgánica, Orgánica y Bioquímica-Centro de Innovación en Química Avanzada (ORFEO-CINQA), Facultad de Ciencias Ambientales y Bioquímica, Universidad de Castilla-La Mancha, 45071 Toledo, Spain*
[c]*Departamento de Química Orgánica e Inorgánica/IUQOEM, Universidad de Oviedo, 33071 Oviedo, Spain*

catalytic approaches under mild conditions is extremely interesting from the perspective of atomic economy.

As in the case of cyclic carbonates, different catalytic systems have been proposed for obtaining oxazolidinones through various coupling reactions, among which the [3 + 2] coupling reaction between isocyanates, nitrogen analogues of CO_2, and epoxides stands out.[5]

Zinc, an abundant and essential element for humans, has emerged as a desirable alternative to scarce metals or organocatalysts, which may pose potential toxicity concerns and limit their use in pharmaceutical applications due to trace contamination.[6]

At present, although numerous zinc-based catalysts have been reported for the synthesis of cyclic carbonates *via* the aforementioned process,[7] systems capable of operating under the more desirable condition of ambient CO_2 pressure are significantly less common (see Table S1).[8]

Moreover, it is noteworthy that, while some zinc compounds have been employed in the synthesis of oxazolidinones, their use in the coupling of epoxides and isocyanates has not yet been reported.[9]

Our group and others have studied zinc guanidinato complexes as potential catalysts in different processes.[10] Guanidinato ligands, $[R_2NC(NR)_2]^-$, allow the stabilization of a wide variety of metals and nonmetals, in addition to sometimes participating in catalytic processes, presenting themselves as an example of metal–ligand cooperation.[11] In this context, we report the use of catalytically synthesized guanidines to prepare and structurally characterize a series of novel zinc guanidinato complexes, aiming to investigate how different donor atoms influence the coordination modes of the ligands. Finally, we examine their multitasking catalytic activity in the coupling of epoxides with either CO_2 or isocyanates (Fig. 1).

Results and discussion

Synthesis of the guanidinato complexes

Recently, we have initiated a systematic study on the potential influence of specific donor groups present as substituents in guanidine-based proligands. Specifically, our aim is to assess the effect of substituents located at the *ortho* position of the aromatic ring derived from the aniline used in guanidine synthesis. We have observed distinct coordination modes depending on whether the guanidines bear softer or harder donor groups, as defined by HSAB theory, and their impact on the catalytic activity of main group metals, namely, magnesium, calcium, or aluminum complexes.[12] Consequently, we sought to extend this investigation to another abundant and even biocompatible metal: zinc.

To prepare the new guanidinato complexes, a direct reaction was carried out between the proligands and a commercial precursor bearing substituents susceptible to protonolysis. This strategy avoids the formation of salt by-products and facilitates the isolation of the desired compound. In this context, the coordination of the proligands, namely $(iPrHN)_2CN(2\text{-}RC_6H_4)$ (R = H **L^{1}H**, F **L^{2}H**, PPh_2 **L^{3}H**, and SPh **L^{4}H**), obtained by a described catalytic process,[10a] to zinc was investigated by treating them with $ZnMe_2$ in a 1 : 1 stoichiometry, leading to the formation of the corresponding guanidinato zinc complexes (see Scheme 1). The reactions were carried out in dry toluene for 10 min at room temperature. After the appropriate workup, complexes **1–4** were obtained in high yields (≥91%) as off-white solids. The use of other proligands with hard -OR or -NR_2-type donor groups proved unsuccessful, giving rise to complex mixtures that appear to contain products resulting from the elimination of these substituent groups from the guanidine. Treatment of the proligands with an excess of $ZnMe_2$ invariably afforded the derivatives depicted in Scheme 1.

The new guanidinato complexes were characterized using spectroscopic techniques and, in some cases, single-crystal X-ray diffraction (details are provided in the SI). The ^{1}H NMR

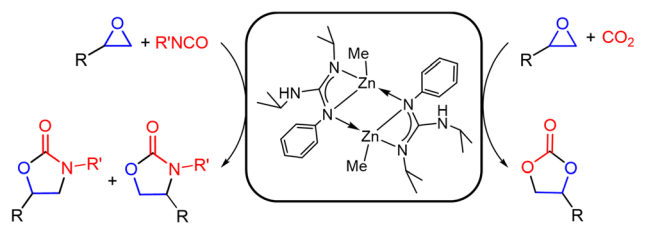

Fig. 1 Catalytic synthesis of cyclic carbonates and oxazolidinones, by coupling of epoxides and CO_2 or isocyanates.

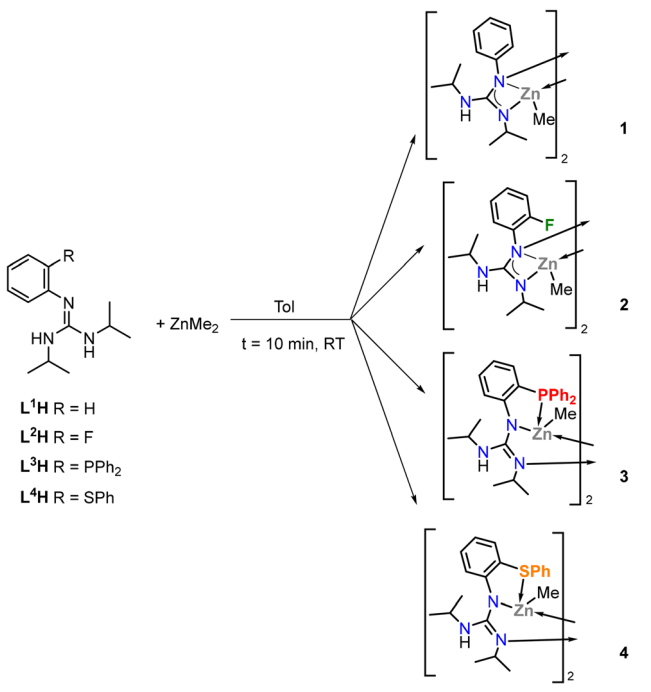

Scheme 1 General pathway for the synthesis of complexes **1–4**, with their proposed structures.

spectra of these complexes in C_6D_6 support their nuclearity relative to the ligands, as evidenced by a signal attributed to the remaining N–H proton of the guanidinato fragment appearing near 3.5 ppm, along with a high field singlet corresponding to the three protons of the ZnMe moiety (see the SI). The methyl groups of the isopropyl substituents on the guanidinato ligands appear differently for complexes **1** and **2** compared to complexes **3** and **4**. In the former case, two doublets were observed, indicating an asymmetric coordination environment for the ligand, which is symmetric in its free form, but with equivalence between the two methyl groups of each isopropyl fragment. In contrast, complexes **4** and **5** display four doublets for these same protons, indicating greater asymmetry in these cases, likely resulting from the chirality around the central atom.

The ^{13}C NMR spectra of compounds **1–4** show a diagnostic peak for the central carbon atom of the guanidinato moiety at approximately 160 ppm across all complexes (see the SI). Additionally, a characteristic signal for the ZnMe group was detected near −10 ppm. In the ^{31}P NMR spectrum of compound **3**, a distinctive peak at −24.2 ppm, shielded with respect to the free ligand signal (see the SI), suggested coordination through the phosphorus atom.[13]

The molecular structures of complexes **3** and **4** were determined by single-crystal X-ray diffraction. Crystals were obtained from toluene/pentane and C_6D_6/pentane solutions, respectively, at −30 °C. The molecular structures are shown in Fig. 2, and a summary of the crystallographic data and data collection parameters is provided in Table S3 in the SI. X-ray diffraction analysis revealed an alternative coordination mode for these two complexes, which may explain the differences observed in their NMR spectra. In both cases, the complexes are dinuclear. The dinuclear core consists of an eight-membered ring formed by two Zn atoms and two N–C–N units from the guanidinato ligands. In fact, each guanidinato ligand coordinates to one Zn atom *via* κ^2-N,P or κ^2-N,S, forming a five-membered chelate ring, and to the other Zn atom through an additional nitrogen atom from the CN_3 core. Regarding this fragment, both complexes exhibit longer N1–C1 (or N1′–C1′) distances (~1.36 Å), where N1 supports the aryl group, compared to the C1–N2 (or C1′–N2′) distances (~1.31 Å). Due to this intermediate hybridization between sp^3 and sp^2 of the N–C bonds in the CN_3 fragment, the metallacycle adopts a distorted boat conformation. This type of coordination has previously been observed in other zinc complexes bearing guanidinato or amidinato ligands.[14] This bridging mode, as alternative to the common chelate coordination mode in most of guanidinato complexes, would agree with the higher bonding tendency between Zn(II), a medium-soft acid, and soft phosphorus or sulfur atoms. In fact, regarding the metal center, it presents a pseudotetrahedral coordination where the guanidinato is coordinated by one N atom and one P or S atom, occupying two positions. The remaining coordination sites are occupied by a methyl group and a nitrogen atom from the guanidinato ligand bound to the other Zn center. This ligand arrangement induces chirality in the complexes, as observed in the NMR studies. Whereas the distances S–Zn in both nuclei are 2.70 Å approximately, the distances P–Zn are 2,59 Å a bit shorter, which highlights its better behavior as Lewis base.

Unfortunately, suitable crystals for diffraction studies could not be obtained for complexes **1** and **2**.[15] Considering the related zinc complex $[Zn(Et)\{(4\text{-}t\text{-}BuC_6H_4)NC(NiPr)(NHiPr)\}]_2$, previously reported by some of us, it is reasonable to propose

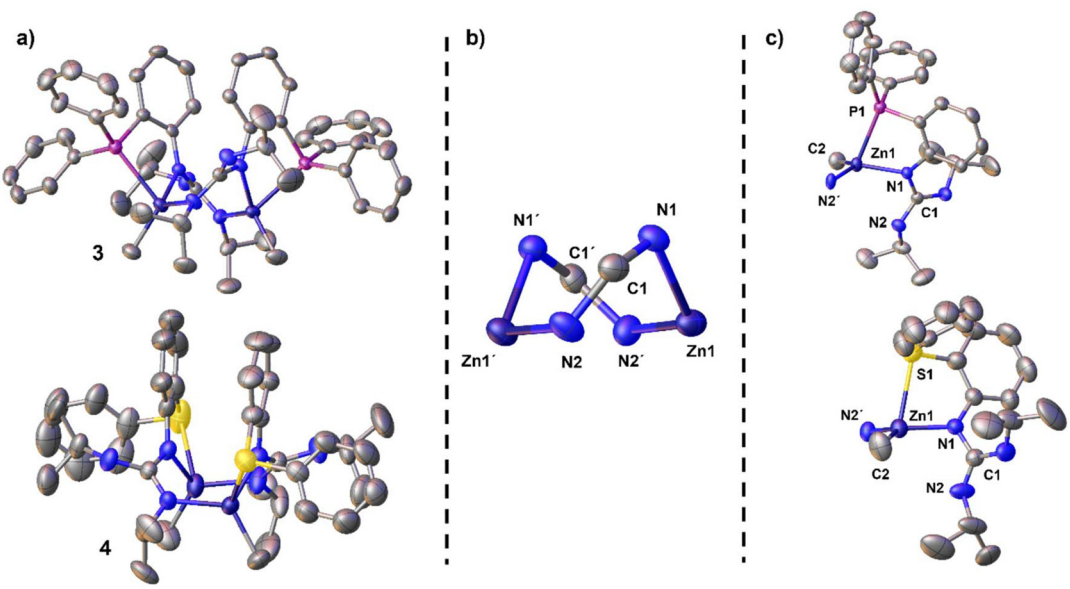

Fig. 2 (a) Full molecular structures of compounds **3** and **4**. (b) View of the metallacycle. (c) Partial view of the coordination around the metal centers. H atoms, solvent molecules and disorder are omitted for clarity.

that both complex **1** and its analogue **2** adopt a similar structure in the solid state.[10a] This dimeric structure features guanidinato ligands coordinated in a chelating κ^2-N,N fashion to each metal center, while also bridging through one of the nitrogen atoms to the metal of the opposite subunit. The alkyl group bound to the metal completes a pseudotetrahedral coordination environment (see Scheme 1). Consequently, DFT calculations at the ωB97X-D/6-311+G(d,p) level for compound **1** clearly support such a structural proposal since a conventional dimeric structure (Fig. 3), with a μ-k^2:k^1-coordination mode of the guanidinato ligands lies nearly 8 kcal mol^{-1} below the corresponding monomer (see SI). It is also worth noting that, as found for $[Zn(Et)\{(4\text{-}t\text{-}BuC_6H_4)NC(NiPr)(NHiPr)\}]_2$, the zinc–nitrogen distance between the two units (*ca.* 2.11 Å) lies between the figures found for the chelate guanidinato ligand (*ca.* 2.05 and 2.29 Å), this suggesting a strong interaction between the monomeric units.

Complex **1** was then analyzed using diffusion-ordered spectroscopy (DOSY, see Fig. S71) which were acquired with the *ledbpgp2s* pulse program.[16] One of the most practical applications of diffusion NMR spectroscopy is the determination of molecular size in solution.[17] This method relies on measuring the diffusion coefficient (D) of the species present in the NMR sample. The diffusion coefficient is a translational property that can be correlated with the hydrodynamic radius (r_h) through the Stokes–Einstein equation.[18] The limitations of this method for heavy atoms and organometallic complexes can be overcome by using the corrections described by Stalke.[19] Using this improved methodology and tetramethylsilane as an internal reference (see SI), a MW_{det} of 572 g mol^{-1} was determined, a value very close to that calculated for a dimeric species (MW_{calc} = 597 g mol^{-1}). This result suggests that this complex maintains its dimeric structure in solution at room temperature.

Catalytic studies for the synthesis of cyclic carbonates

Recently, we reported the use of aluminum guanidinato complexes, which exhibit varying nuclearities and coordination modes. In the presence of appropriate cocatalyst, they efficiently produced a broad range of terminal cyclic carbonates from epoxides bearing diverse functional groups.[20] This all prompted us to explore the reactivity of the new zinc guanidinato complexes as precursors of catalyst for the addition of CO_2 to a range of epoxides.

The catalytic potential of the synthesized complexes was initially evaluated. As a starting point for our investigation, we selected the transformation of styrene oxide (**5a**) into styrene carbonate (**6a**) as a model reaction. The reactions were conducted at 80 °C under 1 bar of CO_2 pressure for 24 hours in toluene, employing 5.0 mol% of complexes **1–4** along with 5.0 mol% of tetrabutylammonium bromide (TBAB) as a co-catalyst. The results are summarized in Table 1. Notably, the unsubstituted guanidinato complex exhibited a higher conversion rate than its congeners (entry 1, Table 1).

For this reason, we focused our attention on the catalytic behavior of complex **1**. Increasing the reaction temperature to 100 °C led to an improved conversion, reaching an excellent 98% (entry 5, Table 1). Reducing the catalyst loading to 1 mol% did not significantly affect the outcome (entry 6, Table 1). We then considered performing the reaction in a more sustainable manner, in the absence of solvent; however, this resulted in a considerable decrease in conversion (entry 7, Table 1). Seeking to maintain these conditions, with a lower catalyst loading and without solvent, we explored the use of an alternative co-catalyst, tetrabutylammonium iodide (TBAI), given that iodide is more nucleophilic than bromide and could potentially enhance epoxide activation. We were pleased to find that, by appropriately adjusting the catalyst-to-co-catalyst ratio to 1 : 2, excellent conversion was achieved under the desired conditions (entry 9, Table 1).

Compared to other zinc-based catalysts that enable the synthesis of cyclic carbonates under a single bar of CO_2 pressure, catalyst **1** demonstrates comparable or even superior performance, with a TON of 91 and a TOF of 3.8 h^{-1} (see Table S1). Given the straightforward synthesis of both the ligand and the

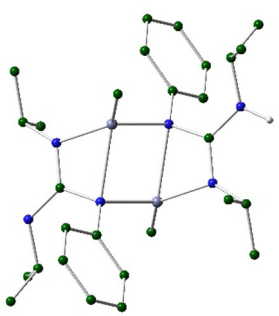

Fig. 3 Optimized structure for complex **1**.

Table 1 Catalytic synthesis of styrene carbonate **6a** employing guanidinato complexes[a]

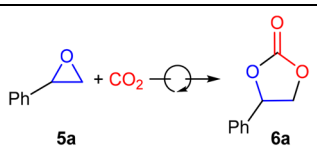

5a **6a**

Entry	Cat	mol% Cat	CoCat (mol%)	t (h)	T (°C)	Conversion[c] (%)
1	**1**	5	Br^- (5)	24	80	71
2	**2**	5	Br^- (5)	24	80	47
3	**3**	5	Br^- (5)	24	80	26
4	**4**	5	Br^- (5)	24	80	50
5	**1**	5	Br^- (5)	24	100	98
6	**1**	1	Br^- (5)	24	100	98
7	**1**[b]	1	Br^- (1)	24	100	50
8	**1**[b]	1	I^- (1)	24	100	83
9	**1**[b]	1	I^- (2)	24	100	91

[a] The reactions were conducted under 1 bar of CO_2 pressure in toluene. [b] Reactions were carried out under solvent free conditions. [c] Conversion was determined by ^{1}H NMR spectroscopy of the reaction mixture relative to starting epoxide.

complex, compound **1** could be an adequate alternative for achieving a more sustainable approach to the formation of these heterocycles.

Thus, with the optimized reaction conditions for the synthesis of compound **6a** established (1 mol% of catalyst **1**, 2.0 mol% of TBAI at 100 °C under 1 bar of CO_2 for 24 hours, in neat conditions), we proceeded to prepare a series of monosubstituted cyclic carbonates (**6a–h**) from their corresponding terminal epoxides (**5a–h**) and carbon dioxide, as illustrated in Fig. 4.

In all cases, the results were outstanding, regardless of the presence of aryl or alkyl substituents on the starting epoxide. The process enables synthesis with an excellent conversion of propylene carbonate **6d**, which is widely used as solvent in lithium-ion batteries.[21] For epichlorohydrin (product **6f**), biomass derived 2-MeTHF was used as a sustainable solvent.[22] Unfortunately, when an internal epoxide such as cyclohexene oxide was used, the reaction led to the formation of the corresponding polycarbonate, a CO_2/epoxide copolymer, *via* ring-opening copolymerization, with an acceptable conversion (see Fig. S28).

Catalytic studies for the synthesis of oxazolidinones

As mentioned in the introduction, there are heterocycles analogous to cyclic carbonates that contain a nitrogen atom in their cyclic core. Oxazolidinones can be synthesized through an alternative catalytic method that has gained attention in recent years, following the development of highly efficient molecular catalysts for the formation of cyclic carbonates. The underlying idea is to replace CO_2 with an isoelectronic analogue, the isocyanate. Therefore, we decided to evaluate the efficiency of catalyst **1** in a coupling reaction between isocyanates and epoxides.

The reaction optimization, summarized in Table 2, was initially based on the conditions established for the previous process, namely, a **1**/TBAI combination with 1 mol% of catalyst and a catalyst/co-catalyst ratio of 1 : 2, at 100 °C, under solvent-free conditions for 24 hours. Styrene oxide and phenyl isocyanate were selected as model substrates. Surprisingly, under these conditions, the reaction did not proceed due to solidifi-

Table 2 Catalytic synthesis of oxazolidinones **8a** and **9a** employing guanidinato complex **1** as catalyst and TBAI as a cocatalyst

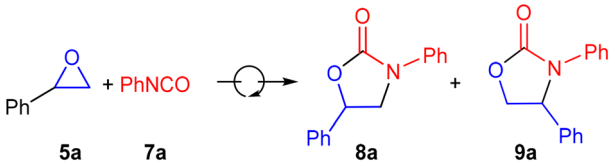

5a **7a** **8a** **9a**

Entry	mol% Cat	mol% CoCat	Conversion[f] (%)	Ratio **8a : 9a**
1[a]	1	2	0	—
2[b]	5	10	85	3.5 : 1
3[c]	5	10	81	3 : 1
4[c]	5	5	74	3.6 : 1
5[c]	2	4	84	2.9 : 1
6[c]	1	2	71	2.3 : 1
7[d]	2	4	77	2.5 : 1
8[e]	2	4	55	2.5 : 1

[a] The reaction was conducted without solvent, at 100 °C for 24 h. [b] Reaction was carried out in toluene (~3 mL). [c] The reactions were conducted in 2-MeTHF (~3 mL). [d] Reaction was carried out at 100 °C for 16 h. [e] Reaction was carried out at 50 °C for 24 h. [f] Conversion was determined by ^{1}H NMR spectroscopy of the reaction mixture relative to starting epoxide.

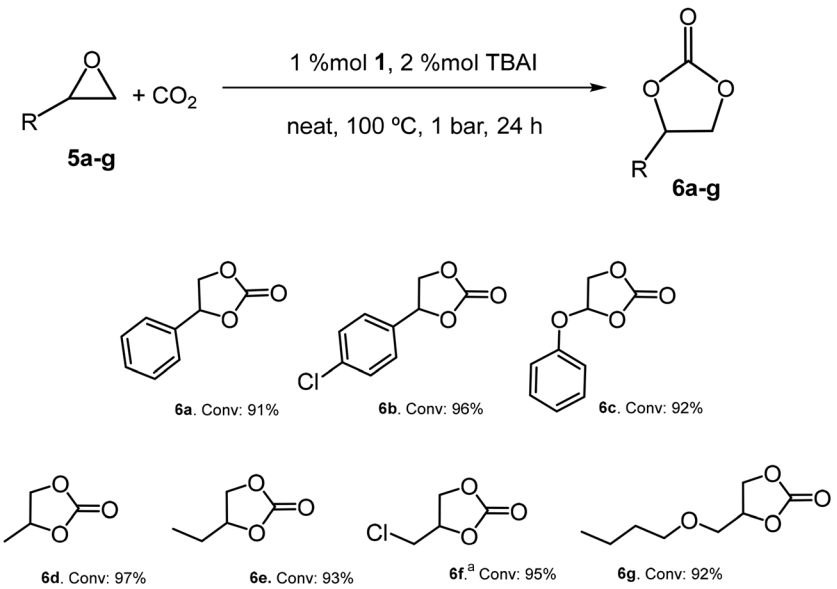

Fig. 4 Synthesis of cyclic carbonates **6a–g**, obtained by using the catalyst system **1**/TBAI. The reactions were carried out in a molar ratio of 1 : 2 cat : cocat (TBAI), at 100 °C and 1 bar of CO_2 pressure for 24 h. Unless stated, were carried out in the absence of solvent. [a]Dry 2-MeTHF was used as solvent. Conversion was determined using ^{1}H NMR spectroscopy of the crude reaction mixture.

cation of the reaction mixture after a short period of time. In contrast, increasing the catalyst loading to 5 mol% and adding a small amount of toluene as solvent enabled an 85% conversion (entry 2, Table 2). The use of the more sustainable solvent 2-MeTHF resulted in a similar conversion (entry 3, Table 2). In fact, a moderate reduction in catalyst loading maintained catalytic activity (entry 5, Table 2). However, further reduction to 1 mol%, or decreasing the amount of co-catalyst, significantly affected the activity (entries 4 and 6, Table 2). A similar decrease in performance was observed when lowering the temperature or shortening the reaction time (entries 7 and 8, Table 2). In all cases, the major product was isomer **8a**, with a near 3 : 1 ratio compared to isomer **9a**.

Based on the results presented in Table 2, entry 5 was selected as the optimal condition for further studies involving various substrates, including both epoxides and isocyanates, leading to the formation of oxazolidinones **8a–i** and **9a–g**, as illustrated in Table 3.

Using styrene oxide as the epoxide and various isocyanates as reactants, a negative correlation between conversion and isocyanate size is observed, as exemplified by derivatives **8b–9b** and **9f**. The presence of electron-withdrawing or mildly electron-donating groups also exerts a moderate negative influence on conversion, as seen in derivatives **8c–e** and **9c–e**. In the case of the *tert*-butyl isocyanate derivative, although the conversion was low, the reaction proceeded regioselectively toward the 3,4-isomer. In contrast, the other cases yield mixtures in which the 3,5-isomer predominates.

To our delight, when phenyl isocyanate was used as the starting reagent and the epoxide varied, yields range from good to excellent. Notably, epoxides bearing alkyl substituents exhibited high regioselectivity toward the 3,5-isomer (compounds **8g–i**). On the contrary, the use of cyclohexene oxide as a substrate only results in traces of the corresponding oxazolidinone.

As was the case with the formation of cyclic carbonates, and in comparison with other catalysts used for the coupling of epoxides and isocyanates,[5] complex **1** exhibits performance that is comparable to or exceeds that of previously described systems, with a turnover number approaching 48 in certain examples (see Table S2).

Computational mechanistic study

Aiming to rationalize the high activity of the dimeric compound **1** in the coupling reactions discussed above, we performed a DFT study of the reaction pathway for the styrene oxide–CO_2 coupling, as a model. In agreement with previous studies on related systems, the calculations support a stepwise mechanism taking place through intermediates that retain the proposed dimeric structure. Thus, the epoxide is first activated by coordination to one of the Zn centers and subsequently undergoes ring-opening by the external halide (I^-). Then CO_2 insertion into the resulting Zn-alkoxide bond followed by ring-closing yields the final cyclic carbonate product. In particular, epoxide coordination to one of the zinc centers in compound **1** (Zn–O = 3.14 Å) takes place with very small energetic penalty

Table 3 Synthesis of oxazolidinones **8a–i** and **9a–g**, obtained by using the catalyst system **1**/TBAI[a,b]

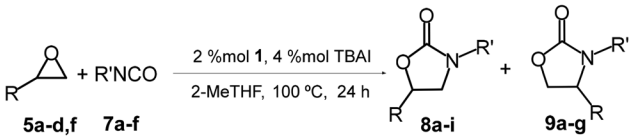

	Conversion (%)	Ratio **8 : 9**
8a + **9a**	84	2.9 : 1
8b + **9b**	32	2.87 : 1
8c + **9c**	55	2.36 : 1
8d + **9d**	70	2.79 : 1
8e + **9e**	72	1.1 : 1
9f	12	0 : 1
8f + **9g**	95	3.65 : 1
8g	69	1 : 0
8h	93	1 : 0
8i	74	1 : 0

[a] The reactions were carried out in a molar ratio of 1 : 2 cat : cocat (TBAI), at 100 °C, in dry 2-MeTHF for 24 h. [b] Conversion was determined using ^{1}H NMR spectroscopy of the crude reaction mixture.

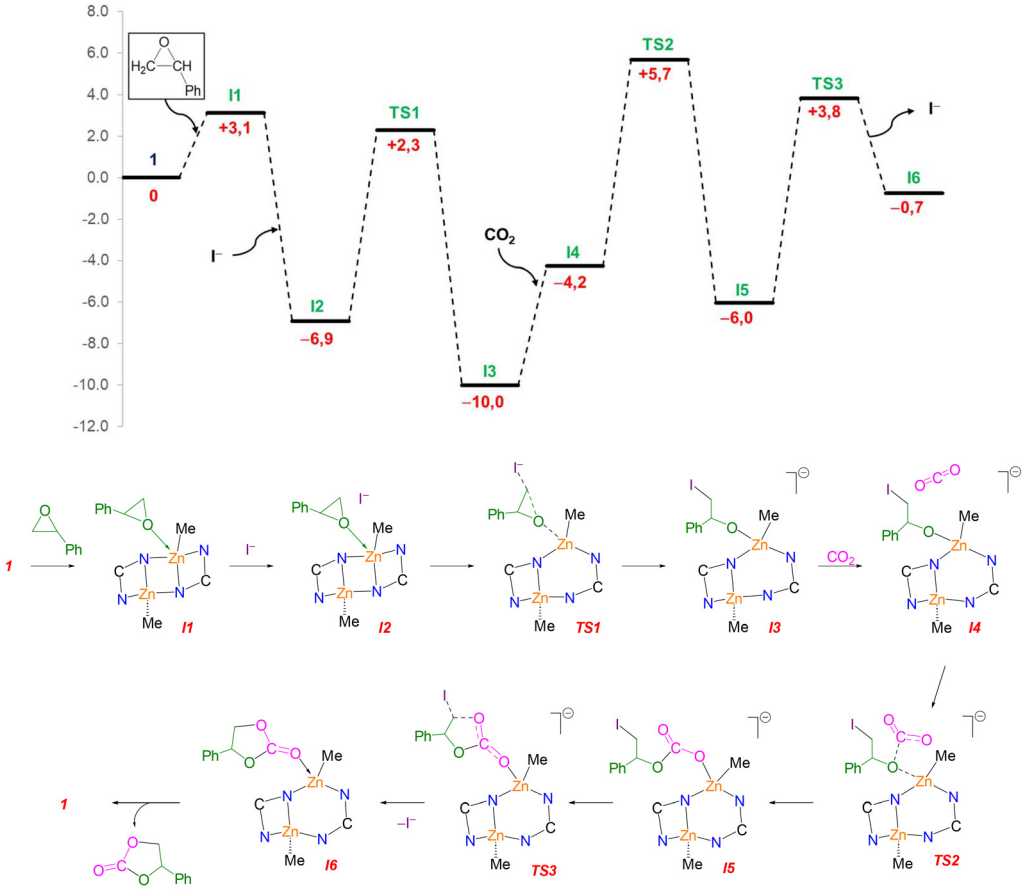

Fig. 5 DFT computed reaction profile for the gas phase styrene oxide-CO_2 coupling catalyzed by compound **1**, with relative Gibbs free expressed in kcal·mol^{-1} (top). Schematic representation of the reaction mechanism with simplified guanidinato ligands (bottom).

(+3.1 kcal mol^{-1}), and without significant distortion of the dimeric motif (intermediate **I1** in Fig. 5). Iodide attack at the CH_2 group of the Lewis-activated epoxide proceeds readily, with an energy barrier of only 9.2 kcal mol^{-1}, thereby yielding a low-energy zinc alkoxide intermediate (**I3**, Zn–O = 1.99 Å). Interestingly, although this latter intermediate preserves a dinuclear structural motif, the guanidinato ligands adopt markedly different coordination modes (μ-k^1:k^1 and μ-k^2:k^1, respectively). This rearrangement, in which one unit of the dinuclear complex acts as a metalloligand, provides a more open framework (distorted 6-membered ring), which accommodates the zinc center bearing the alkoxide group. Subsequent nucleophilic attack of the alkoxide on the CO_2 molecule occurs *via* transition state **TS2**, located *ca.* 16 kcal mol^{-1} above **I3**, constituting the rate-limiting step of the catalytic cycle. Finally, concerted carbonate ring closure and halide elimination take place with an activation barrier of *ca.* 9 kcal mol^{-1}, leading to intermediate **I6**, in which the newly formed cyclic carbonate remains coordinated to the metal center. Overall, while the dimeric structure is preserved throughout the pathway, the coordination flexibility of the guanidinato ligands in **1** appears to be a key factor in facilitating the coupling process by allowing efficient adaptation to the particular demands of the Zn centers along the process.

Conclusions

The search for new homogeneous catalysts for the synthesis of heterocycles of interest, such as cyclic carbonates and oxazolidinones, is focused on employing more efficient catalysts under mild reaction conditions, with high selectivity, while adhering to sustainability principles and minimizing environmental impact. Zinc-based catalysts represent a promising option to meet these challenges. In this work, we describe and characterize a series of organometallic complexes based on this metal and guanidinato ligands. This approach has enabled the identification of a simple catalyst capable of producing cyclic carbonates of interest from epoxides and CO_2 at atmospheric pressure, achieving excellent yields. Furthermore, the multitasking ability of this catalyst has been demonstrated, as it also facilitates the synthesis of a wide range of oxazolidinones, with good to very good yields, through the coupling of epoxides and isocyanates. Based on density functional theory

calculations, a plausible mechanism for the cyclization process has been proposed.

Author contributions

Fernando Carrillo-Hermosilla: conceptualization, funding acquisition, project administration, supervision, visualization, writing – review & editing. Alberto Ramos: conceptualization, writing – review. Daniel García-Vivó: formal analysis, writing – original draft preparation. David Elorriaga: investigation, writing – original draft preparation. Rafael Fernández-Galán: investigation, writing – original draft preparation. Blanca Parra-Cadenas: investigation, data curation, writing – original draft preparation. Carlos Ginés: investigation, data curation, writing – original draft preparation.

Conflicts of interest

There are no conflicts to declare.

Data availability

The data supporting this article have been included as the supplementary information (SI). Supplementary information is available. See DOI: https://doi.org/10.1039/d6dt00139d.

CCDC 2520691 (**1′**), 2520689 (**3**) and 2520690 (**4**) contain the supplementary crystallographic data for this paper.[23a–c]

Acknowledgements

We gratefully acknowledge financial support from MICIU/AEI /10.13039/501100011033 (Project numbers PID2020-117353GB-I00, PID2021-123964NB-I00 and RED2022-134287-T), from JCCM and EU through Fondo Europeo de Desarrollo Regional, FEDER (Project number SBPLY/23/180225/000021), the Universidad de Castilla-La Mancha (Project number 2025-GRIN-38435), and the SCBI (Supercomputer and Bioinformatics) center of the University of Málaga (Spain) for access to computing facilities.

References

1 (*a*) I. Omae, *Coord. Chem. Rev.*, 2012, **256**, 1384–1405; (*b*) M. Aresta, A. Dibenedetto and A. Angelini, *J. CO_2 Util.*, 2013, **3**, 65–73; (*c*) M. Aresta, A. Dibenedetto and A. Angelini, *Chem. Rev.*, 2013, **114**, 1709–1742; (*d*) C. Maeda, Y. Miyazaki and T. Ema, *Catal. Sci. Technol.*, 2014, **4**, 1482–1497; (*e*) J. Artz, T. E. Müller, K. Thenert, J. Kleinekorte, R. Meys, A. Sternberg, A. Bardow and W. Leitner, *Chem. Rev.*, 2018, **118**(2), 434–504.

2 (*a*) C. Martín, G. Fiorani and A. W. Kleij, *ACS Catal.*, 2015, **5**, 1353–1370; (*b*) P. P. Pescarmona, *Curr. Opin. Green Sustainable Chem.*, 2021, **29**, 100457; (*c*) G. A. Bhat and D. J. Darensbourg, *Green Chem.*, 2022, **24**, 5007–5034; (*d*) T. Sakakura and K. Kohno, *Chem. Commun.*, 2009, 1312–1330; (*e*) L. Guo, K. J. Lamb and M. North, *Green Chem.*, 2021, **23**, 77–118; (*f*) V. Mishra and S. C. Peter, *Chem. Catal.*, 2023, **4**, 100796; (*g*) F. Zhang, Y. Wang, X. Zhang, X. Zhang, H. Liu and B. Han, *Green Chem. Eng.*, 2020, **1**, 82–93; (*h*) V. Aomchad, A. Cristofol, F. Della Monica, B. Limburg, V. D'Elia and A. W. Kleij, *Green Chem.*, 2021, **23**, 1077–1113.

3 (*a*) C. Foti, A. Piperno, A. Scala and O. Giuffrè, *Molecules*, 2021, **26**, 4280–4293; (*b*) N. Pandit, R. K. Singla and B. Shrivastava, *Int. J. Med. Chem.*, 2012, 159285; (*c*) M. R. Barbachyn and C. W. Ford, *Angew. Chem., Int. Ed.*, 2003, **42**, 2010–2023.

4 F. Sun, E. V. Van der Eycken and H. Feng, *Adv. Synth. Catal.*, 2021, **363**, 5168–5195.

5 (*a*) J. E. Herweh and W. J. Kauffman, *Tetrahedron Lett.*, 1971, **12**, 809–812; (*b*) I. Shibata, A. Baba, H. Iwasaki and H. Matsuda, *J. Org. Chem.*, 1986, **51**, 2177–2184; (*c*) A. Baba, M. Fujiwara and H. Matsuda, *Tetrahedron Lett.*, 1986, **27**, 77–80; (*d*) C. Qian and D. Zhu, *Synlett*, 1994, 129–130; (*e*) L. Aroua and A. Baklouti, *Synth. Commun.*, 2007, **37**, 1935–1942; (*f*) M. T. Barros and A. M. Faísca Phillips, *Tetrahedron: Asymmetry*, 2010, **21**, 2746–2752; (*g*) T. Baronsky, C. Beattie, R. W. Harrington, R. Irfan, M. North, J. G. Osende and C. Young, *ACS Catal.*, 2013, **3**, 790–797; (*h*) R. L. Paddock, D. Adhikari, R. L. Lord, M.-H. Baik and S. T. Nguyen, *Chem. Commun.*, 2014, **50**, 15187–15190; (*i*) C. Beattie and M. North, *RSC Adv.*, 2014, **4**, 31345–31352; (*j*) P. Wang, J. Qin, D. Yuan, Y. Wang and Y. Yao, *ChemCatChem*, 2015, **7**, 1145–1151; (*k*) J. A. Castro-Osma, A. Earlam, A. Lara-Sánchez, A. Otero and M. North, *ChemCatChem*, 2016, **8**, 2100–2108; (*l*) X. Wu, J. Mason and M. North, *Chem. – Eur. J.*, 2017, **23**, 12937–12943; (*m*) Y. Toda, S. Gomyou, S. Tanaka, Y. Komiyama, A. Kikuchi and H. Suga, *Org. Lett.*, 2017, **19**, 5786–5789; (*n*) M. Yang, N. Pati, G. Bélanger-Chabot, M. Hirai and F. P. Gabbaï, *Dalton Trans.*, 2018, **47**, 11843–11850; (*o*) H. J. Altmann, M. Clauss, S. König, E. Frick-Delaittre, C. Koopmans, A. Wolf, C. Guertler, S. Naumann and M. R. Buchmeiser, *Macromolecules*, 2019, **52**, 487–494; (*p*) Y. Toda, S. Tanaka, S. Gomyou, A. Kikuchi and H. Suga, *Chem. Commun.*, 2019, **55**, 5761–5764; (*q*) P. Yingcharoen, W. Natongchai, A. Poater and V. D'Elia, *Catal. Sci. Technol.*, 2020, **10**, 5544–5558; (*r*) R. Nishiyori, K. Okuno and S. Shirakawa, *Eur. J. Org. Chem.*, 2020, 4937–4941; (*s*) A. Rostami, A. Ebrahimi, J. Husband, M. U. Anwar, R. Csuk and A. Al-Harrasi, *Eur. J. Org. Chem.*, 2020, 1881–1895; (*t*) D.-X. Cui, Y.-D. Li, P. Huang, Z. Tian, Y.-Y. Jia and P.-A. Wang, *RSC Adv.*, 2020, **10**, 12360–12364; (*u*) A. Rostami, A. Ebrahimi, N. Sakhaee, F. Golmohammadi and A. Al-Har, *J. Org. Chem.*, 2022, **87**, 40–55; (*v*) M. P. Caballero, F. Carrascosa, F. de la Cruz-Martínez, J. A. Castro-Osma, A. M. Rodríguez, M. North, A. Lara-Sánchez and J. Tejeda, *ChemistrySelect*, 2022, **7**,

e202103977; (*w*) Z. Zhang, Y. Ni, Z. Li, J. He, X. Zou, X. Yuan, Z. Liu, S. Cao, C. Ma and K. Guo, *Mol. Catal.*, 2023, **548**, 113425.

6 (*a*) S. Enthaler, *ACS Catal.*, 2013, **3**, 150–158; (*b*) S. Enthaler and X.-F. Wu, *Zinc Catalysis: Applications in Organic Synthesis*, Wiley-VCH Verlag GmbH & Co. KGaA, Weinheim, 2015; (*c*) M. S. Holzwarth and B. Plietker, *ChemCatChem*, 2013, **5**, 1650–1679.

7 D. Prasad, K. N. Patil, N. K. Chaudhari, H. Kim, B. M. Nagaraja and A. H. Jadhav, *Catal. Rev.*, 2020, **64**(2), 356–443.

8 (*a*) Y. Yang, Y. Hayashi, Y. Fujii, T. Nagano, Y. Kita, T. Ohshima, J. Okuda and K. Mashima, *Catal. Sci. Technol.*, 2012, **2**(3), 509–513; (*b*) H. V. Babu and K. Muralidharan, *Dalton Trans.*, 2013, **42**(4), 1238–1248; (*c*) X.-D. Lang, Y.-C. Yu and L.-N. He, *J. Mol. Catal. A: Chem.*, 2016, **420**, 208–215; (*d*) L. Cuesta-Aluja, A. Campos-Carrasco, J. Castilla, M. Reguero, A. M. Masdeu-Bultó and A. Aghmiz, *J. CO_2 Util.*, 2016, **14**, 10–22; (*e*) S. He, F. Wang, W.-L. Tong, S.-M. Yiu and M. C. W. Chan, *Chem. Commun.*, 2016, **52**(7), 1017–1020; (*f*) C. Maeda, J. Shimonishi, R. Miyazaki, J. Hasegawa and T. Ema, *Chem. – Eur. J.*, 2016, **22**(19), 6556–6563; (*g*) Y. Ge, G. Cheng, N. Xu, W. Wang and H. Ke, *Catal. Sci. Technol.*, 2019, **9**, 4255–4261; (*h*) S. Zhang, F. Han, S. Yan, M. He, C. Miao and L.-N. He, *Eur. J. Org. Chem.*, 2019, 1311–1316; (*i*) J.-J. Chen, Y.-C. Xu, Z.-L. Gan, X. Peng and X.-Y. Yi, *Eur. J. Inorg. Chem.*, 2019, 1733–1739; (*j*) S. Sobrino, M. Navarro, J. Fernández-Baeza, L. F. Sánchez-Barba, A. Garcés, A. Lara-Sánchez and J. A. Castro-Osma, *Dalton Trans.*, 2019, **48**(28), 10733–10742; (*k*) G. Chen, J. Zhang, X. Cheng, X. Tan, J. Shi, D. Tan, B. Zhang, Q. Wan, F. Zhang, L. Liu, B. Han and G. Yang, *ChemCatChem*, 2020, **12**(7), 1963–1967; (*l*) F. M. Al-Qaisi, A. K. Qaroush, A. H. Smadi, F. Alsoubani, K. I. Assaf, T. Repo and A. F. Eftaiha, *Dalton Trans.*, 2020, **49**, 7673–7679; (*m*) R. Kumar, S. C. Sahoo and P. K. Nanda, *Eur. J. Inorg. Chem.*, 2021, 1057–1064; (*n*) K. I. Assaf, A. K. Qaroush, I. K. Okashah, F. M. Al-Qaisi, F. Alsoubani and A. F. Eftaiha, *React. Chem. Eng.*, 2021, **6**, 2364–2375; (*o*) K. Naveen, H. Ji, T. S. Kim, D. Kim and D.-H. Cho, *Appl. Catal., B*, 2021, **280**, 119395; (*p*) K. Yin, L. Hua, L. Qu, Q. Yao, Y. Wang, D. Yuan, H. You and Y. Yao, *Dalton Trans.*, 2021, **50**(4), 1453–1464; (*q*) J. Ma, Y. Wu, X. Yan, C. Chen, T. Wu, H. Fan, Z. Liu and B. Han, *Phys. Chem. Chem. Phys.*, 2022, **24**(7), 4298–4304; (*r*) M. Navarro, S. Sobrino, I. Fernández, A. Lara-Sánchez, A. Garcés and L. F. Sánchez-Barba, *Dalton Trans.*, 2024, **53**, 13933–13949.

9 (*a*) X. Liu, M.-Y. Wang, S.-Y. Wang, Q. Wang and L.-N. He, *ChemSusChem*, 2017, **10**, 1210–1216; (*b*) Y. Chen, R. Luo, Z. Yang, X. Zhou and H. Ji, *Sustainable Energy Fuels*, 2018, **2**, 125–132.

10 (*a*) C. Alonso-Moreno, F. Carrillo-Hermosilla, A. Garcés, A. Otero, I. López-Solera, A. M. Rodriguez and A. Antiñolo, *Organometallics*, 2010, **29**(12), 2789–2795; (*b*) M. K. Barman, A. Baishya and S. Nembenna, *J. Organomet. Chem.*, 2015, **785**, 52–60; (*c*) J. Börner, S. Herres-Pawlis and U. Flörke, *Eur. J. Inorg. Chem.*, 2007, 5645–5651; (*d*) S. D. Bunge, J. M. Lance and J. A. Bertke, *Organometallics*, 2007, **26**, 6320–6328; (*e*) R. K. Sahoo, A. G. Patro, N. Sarkar and S. Nembenna, *Organometallics*, 2023, **42**(14), 1746–1758; (*f*) R. K. Sahoo, N. Sarkar and S. Nembenna, *Inorg. Chem.*, 2023, **62**, 304–317; (*g*) I. D'Auria, V. Ferrara, C. Tedesco, W. Kretschmer, R. Kempe and C. Pellecchia, *ACS Appl. Polym. Mater.*, 2021, **3**, 4035–4043; (*h*) M. P. Coles and P. B. Hitchcock, *Eur. J. Inorg. Chem.*, 2004, 2662–2672; (*i*) M. Fuchs, M. Walbeck, E. Jagla, A. Hoffmann and S. Herres-Pawlis, *ChemPlusChem*, 2022, **11**, e202200029; (*j*) J. Börner, U. Flörke, T. Glöge, T. Bannenberg, M. Tamm, M. D. Jones, A. Döring, D. Kuckling and S. Herres-Pawlis, *J. Mol. Catal. A: Chem.*, 2010, **316**, 139–145; (*k*) J. Li, J. Shi, H. Han, Z. Guo, H. Tong, X. Wei, D. Liu and M. F. Lappert, *Organometallics*, 2013, **32**, 3721–3727.

11 (*a*) A. Gómez-Torres, D. Sengupta and S. Fortier, in *Compr. Coord. Chem. III*, ed. E. C. Constable, G. Parkin and L. Que, Elsevier, Amsterdam, 2021, vol. 3, pp. 366–405; (*b*) C. Alonso-Moreno, A. Antiñolo, F. Carrillo-Hermosilla and A. Otero, *Chem. Soc. Rev.*, 2014, **43**, 3406–3425; (*c*) F. Carrillo-Hermosilla, R. Fernández-Galán, A. Ramos and D. Elorriaga, *Molecules*, 2022, **27**, 5962–5993.

12 (*a*) C. Ginés, B. Parra-Cadenas, R. Fernández-Galán, D. García-Vivó, D. Elorriaga, A. Ramos and F. Carrillo-Hermosilla, *Adv. Synth. Catal.*, 2025, **367**, e202400843; (*b*) C. Ginés, B. Parra-Cadenas, R. Fernández-Galán, D. Elorriaga, A. Ramos, D. García-Vivó and F. Carrillo-Hermosilla, *Adv. Synth. Catal.*, 2026, **368**, e70177.

13 J. Huang, X. Zheng, I. Del Rosal, B. Zhao, L. Maron and X. Xu, *Inorg. Chem.*, 2020, **59**, 13473–13480.

14 (*a*) Ref. 10k (*b*) A. Martínez, S. Moreno-Blázquez, A. Rodríguez-Diéguez, A. Ramos, R. Fernández-Galán, A. Antiñolo and F. Carrillo-Hermosilla, *Dalton Trans.*, 2017, **46**, 12923–12934.

15 In one attempt to determine the molecular structure of complex **1**, crystals suitable for X-ray diffraction were successfully formed. Surprisingly, the resulting structure revealed a saddle-shaped dimeric molecule **1′** featuring a planar Zn_2O_2 metallacycle, formed through reaction with adventitious oxygen. This led to the formation of an N,O-type ligand via insertion of an oxygen atom between the nitrogen atom bearing the aromatic group and the metal center (see Fig. S72).

16 (*a*) K. F. Morris and C. S. Johnson Jr, *J. Am. Chem. Soc.*, 1992, **114**, 3139–3141; (*b*) C. S. Johnson Jr, *Prog. Nucl. Magn. Reson. Spectrosc.*, 1999, **34**, 203–256; (*c*) D. W. T. Claridge, in *High Resolution NMR Techniques in Organic Chemistry*, Elsevier Ed., Oxford, 2nd edn, 2009, ch 9, Tetrahedron Organic Chemistry Series.

17 (*a*) S. Viel, L. Mannina and A. Segre, *Tetrahedron Lett.*, 2002, **43**, 2515–2519; (*b*) M. D. Díaz and S. Berger, *Carbohydr. Res.*, 2000, **329**, 1–5; (*c*) I. Keresztes and P. G. Williard, *J. Am. Chem. Soc.*, 2000, **122**, 10228–10229; (*d*) X. Ribas,

J. C. Dias, J. Morgado, K. Wurst, M. Almeida, T. Parella, J. Veciana and C. Rovira, *Angew. Chem., Int. Ed.*, 2004, **43**, 4049–4052; (*e*) N. Schlörer, E. J. Cabrita and S. Berger, *Angew. Chem., Int. Ed.*, 2002, **41**, 107–109.

18 Stokes–Einstein equation: $D=K_BT/6\pi\eta r_H$, (D=diffusion coefficient, K_B=Boltzman constant, η=solvent viscosity, r_H=hydrodynamic radius).

19 (*a*) S. Bachmann, B. Gernert and D. Stalke, *Chem. Commun.*, 2016, **52**, 12861–12864; (*b*) R. Neufeld and D. Stalke, *Chem. Sci.*, 2015, **6**, 3354–3364; (*c*) S. Bachmann, R. Neufeld, M. Dzemski and D. Stalke, *Chem. – Eur. J.*, 2016, **22**, 8462–8465.

20 Y. R. Yepes, Á. Mesías-Salazar, A. Becerra, C. G. Daniliuc, A. Ramos, R. Fernández-Galán, A. Rodríguez-Diéguez, A. Antiñolo, F. Carrillo-Hermosilla and R. S. Rojas, *Organometallics*, 2021, **40**, 2859–2869.

21 (*a*) M. Wakihara and O. Yamamoto, *Lithium Ion Batteries: Fundamentals and Performance*, Kodansha Ltd., Tokyo, 1998; (*b*) B. Schäffner, F. Schäffner, S. P. Verevkin and A. Börner, *Chem. Rev.*, 2010, **110**(8), 4554–4581.

22 K. Dalvand, J. Rubin, S. Gunukula, M. C. Wheeler and G. Hunt, *Biomass Bioenergy*, 2018, **115**, 56–63.

23 (*a*) CCDC 2520691: Experimental Crystal Structure Determination, 2026, DOI: 10.5517/ccdc.csd.cc2qlzmy; (*b*) CCDC 2520689: Experimental Crystal Structure Determination, 2026, DOI: 10.5517/ccdc.csd.cc2qlzkw; (*c*) CCDC 2520690: Experimental Crystal Structure Determination, 2026, DOI: 10.5517/ccdc.csd.cc2qlzlx.